Variability of central United States April–May tornado day likelihood by phase of the Madden-Julian Oscillation

Bradford S. Barrett[1] and Victor A. Gensini[2]

Received 18 March 2013; revised 28 April 2013; accepted 29 April 2013; published 6 June 2013.

[1] April–May tornado day likelihood from 1990 to 2011 was calculated for the central United States for phases of the Madden-Julian Oscillation (MJO). An April tornado day was found more likely during MJO phases 6 and 8 and less likely during phases 3, 4, and 7. A May tornado day was found more likely during phases 5 and 8 and less likely in phases 2 and 3. During phases with above-normal tornado day likelihoods, positive anomalies of convective available potential energy, bulk vertical wind shear, and storm-relative helicity were found in the central United States. Negative anomalies were found during phases with below-normal tornado day likelihoods. Anomalies of such environmental parameters were connected to the MJO via variability in tropospheric circulation. These results provide an important starting point for extended range prediction of U.S. tornado activity. **Citation:** Barrett, B. S., and V. A. Gensini (2013), Variability of central United States April–May tornado day likelihood by phase of the Madden-Julian Oscillation, *Geophys. Res. Lett.*, *40*, 2790–2795, doi:10.1002/grl.50522.

1. Introduction

[2] The prediction of small-scale weather features, such as tornadoes, remains a challenging task, even though large-scale atmospheric patterns favorable for tornado activity, including the presence of a midtropospheric and upper tropospheric trough, low static stability, high surface water vapor mixing ratios, and the positioning of features, such as low-level jets, fronts, and the dry line, have been well known for decades [*Fawbush et al*., 1951; *Lee and Galway*, 1956; *Kloth and Davies-Jones*, 1980; *Schaefer*, 1986; *Doswell*, 1987; *Thompson and Edwards*, 2000; *Brooks et al*., 2003a]. Local conditions favorable for tornado formation have also been well documented, including high levels of convective available potential energy (CAPE), 0–6 km bulk vertical wind shear [*Rasmussen and Blanchard*, 1998; *Craven et al*., preprint, 2002; *Rasmussen*, 2003], and 0–3 km storm-relative helicity (SRH) [*Davies-Jones et al*., preprint, 1990]. What is not yet well known is how these parameters vary on climate time scales [*Cook and Shaeffer*, 2008; *Tippett et al*., 2012], thereby affecting tornado occurrence. The focus of this study was to examine the projection of the leading planetary scale mode of intraseasonal variability, the Madden-Julian Oscillation (MJO) [*Madden and Julian*, 1971] onto U.S. tornado activity.

[3] The MJO has been shown to modulate a broad range of weather phenomena in the United States, including lower, middle, and upper tropospheric circulation [*Seo and Son*, 2012; *Roundy et al*., 2010; *Lorenz and Hartmann*, 2006]; surface temperature [*Zhou et al*., 2011; *Yao et al*., 2011]; daily rainfall [*Becker et al*., 2011; *Jones et al*., 2011; *Zhou et al*., 2011; *Donald et al*., 2006]; and cloud-to-ground lightning [*Abatzoglou and Brown*, 2009]. As Rossby waves propagate northeastward [e.g., *Wang and Rui*, 1990; *Waliser*, 2006] and downstream [*Gottschalck et al*., 2010] from anomalous equatorial convection associated with the MJO, the form and shape of the resulting wave train depends strongly on the longitudinal center of the heating [*Matthews et al*., 2004]. As this MJO-modulated wave train reaches the United States, it projects onto local conditions [*Zhang*, 2013], including those that impact tornado activity. This modulation of local atmospheric parameters, specifically CAPE, 0–6 km bulk shear, and 0–3 km SRH, and their further downscale controls of tornado activity, was the focus of this study.

2. Data and Methods

[4] Tornado activity for April–May 1990–2011 was determined by converting the tornado data set, which lists the date, time, location, and (if known) intensity and damage of each tornado verified in the United States [*Schaefer and Edwards*, preprints, 1999; *McCarthy*, preprints, 2003, available and described online at http://www.spc.noaa.gov/wcm/#data] into binary form. Days in which at least one tornado occurred in the central United States, defined as an area roughly bounded by the Rocky Mountains and the Mississippi River (specifically east of 106°W and west of 90°W), were classified as tornado days. This method, along with the period 1990–2011, was chosen in an effort to mitigate the well-documented, nonmeteorological increase in tornado reports associated with population growth and changes in observing technology and reporting policy [*Brooks et al*., 2003b; *Doswell et al*., 2005; *Verbout et al*., 2006]. Because the likelihood of a tornado day increases between early April and late May, those months were treated separately. The tornado day data set was binned by phase of the MJO, where phase was determined using the Real-time Multivariate MJO (RMM) index [*Wheeler and Hendon*, 2004]. The RMM index is divided into eight phases, each corresponding to the broad location of an MJO-enhanced equatorial convective signal. The index is created such that the MJO generally progresses eastward, from phases 1 to 8 and back to phase 1 again. Only active MJO days were considered for this study, and an active MJO day was defined as one where the root sum of the two squared principal components,

[1]Oceanography Department, U.S. Naval Academy, Annapolis, Maryland, USA.
[2]Meteorology Program, College of DuPage, Glen Ellyn, Illinois, USA.

Corresponding author: B. S. Barrett, Oceanography Department, U.S. Naval Academy, 572C Holloway Rd., Annapolis, MD 21402, USA. (bbarrett@usna.edu)

0094-8276/13/10.1002/grl.50522

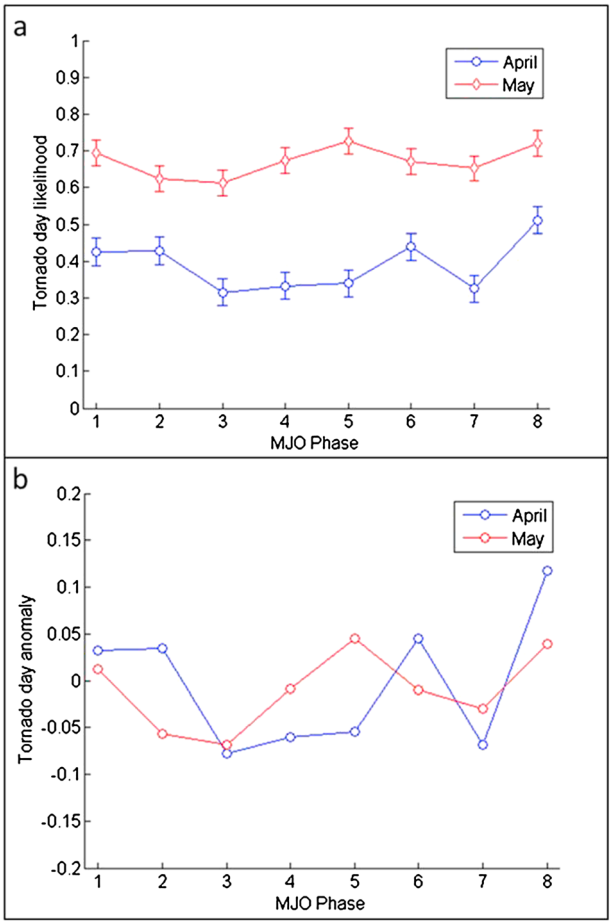

Figure 1. (a) Likelihood and (b) anomaly of a central U.S. tornado day, between 90°W and 106°W by MJO Phase, April and May 1990–2011. Error bars in Figure 1a indicate 95% confidence intervals.

RMM1 and RMM2, was greater than one [following the methodology of *Barrett et al.*, 2012a]. Tornado day likelihood for each MJO phase was found by dividing the number of tornado days in a phase by the total number of days in that phase. Anomalies for each phase were then calculated by subtracting the likelihood of a tornado day for the month from the likelihood of a tornado day for that particular phase. Anomalies were calculated separately for April and May. Statistical significance was computed for each month and MJO phase using a binary test. The z statistic in this test was calculated using

$$\frac{z_i = \hat{p}_i - p_0}{(p_0)(1-p_0)/\sqrt{N}}$$

where z_i is the z statistic for the ith phase of the MJO, $\hat{p}_i$ the probability of a tornado day in the ith MJO phase, N the number of days in the sample, and p_0 the probability of a tornado day on any day in April or May.

[5] Composite anomalies of CAPE, 0–6 km bulk shear, and 0–3 km SRH, variables known to be good discriminators of tornado activity [*Rasmussen and Blanchard*, 1998; *Rasmussen*, 2003], were calculated for each MJO phase using the North American Regional Reanalysis (NARR) [*Mesinger and Coauthors*, 2006]. Composite anomalies of 500 hPa height, 850 hPa height, and sea level pressure were also calculated for each MJO phase to show low-frequency variability of circulation by MJO phase. NARR data were provided on a 32 km Lambert grid in 3 h intervals. CAPE and 0–3 km SRH were obtained directly from the NARR archives, while bulk 0–6 km vertical wind difference (also called "0–6 km bulk wind shear") was found by vertically interpolating winds at constant pressure levels to above-ground level (AGL) height coordinates following the methodology of *Gensini and Ashley* [2011]. Anomalies of daily April–May CAPE, 0–6 km bulk shear, 0–3 km SRH, 500 hPa height, 850 hPa height, and mean sea level pressure were found at 0000 UTC for each MJO phase by subtracting the mean overall values of each parameter from the mean values of each parameter composited by MJO phase. Additionally, the product of CAPE and 0–6 km bulk wind difference (normalized by 20,000) was examined, as it is also considered to be a physically meaningful parameter for characterizing tornado environments [*Brooks et al.*, 2003a; *Doswell and Schultz*, 2006]. Statistical significance at each grid point for each MJO phase was calculated using the Mann-Whitney U test for the medians. Finally, the 0000 UTC hour was chosen because convective parameters typically reach a daily maximum around that hour, and because most tornado activity occurs in the hours around local sunset [*Kelly et al.*, 1978].

3. Results

3.1. Tornado Day Likelihood

[6] From 1990 to 2011, the likelihood of a tornado day in the central United States between 90°W and 106°W was 0.39 in April and 0.68 in May. This likelihood was found to vary by MJO phase (Figure 1). For example, on days when the MJO was in phase 8, the likelihood of a tornado day increased to 0.51 in April (0.12 above normal) and 0.72 in May (0.04 above normal) (Table 1). Phase 8 was the only phase with statistically significant above-normal likelihoods of a tornado day in both April and May (Table 1, p values for each phase are provided). The likelihood of a tornado day in April was statistically significantly below normal in MJO phases 3–5 and 7, with anomalies ranging from −0.05 to −0.08. In May, likelihood of a tornado day was statistically significantly below normal in phases 2 and 3, with anomalies of −0.06 to −0.07, respectively. The likelihood of a tornado day in April during phase 6 was 0.44 or 0.05 above normal. In May, the likelihood of a tornado day during phase 5 was 0.73 or 0.05 above normal. These above-normal likelihoods of a tornado in phase 6 (April) and phase 5 (May) were statistically significant at the 95% confidence level (Table 1).

3.2. CAPE, Shear, and Helicity

[7] Composite anomalies of CAPE, bulk vertical wind shear, and SRH were examined for each MJO phase to see if the larger scale environment supported the observed variability in tornado days. In April, mostly positive CAPE anomalies, up to 500 J kg^{-1} above normal, occurred in phases 5–8, while negative anomalies, as much as 500 J kg^{-1} below normal, occurred in phases 1–4 (Figure 2, row 1). This pattern agreed with the tornado day anomalies, whereby tornado days were more likely during phases 6 and 8, when CAPE was above normal, and less likely during phases 3 and 4, when CAPE was below normal. In addition to CAPE, bulk vertical wind shear also varied by MJO phase

Table 1. Tornado Day Statistics and Likelihood[a]

April Tornadoes	MJO Phase							
	1	2	3	4	5	6	7	8
Number of tornado days	20	15	12	19	18	18	13	22
Total number of days	47	35	38	57	53	41	40	43
Tornado day likelihood ($\bar{x}$ = 0.39)	0.43	0.43	0.32	0.33	0.34	0.44	0.33	0.51
Tornado day anomaly	0.03	0.03	**−0.08**	**−0.06**	**−0.05**	**0.05**	**−0.07**	**0.12**
p Value	0.10	0.07	0.00	0.00	0.00	0.02	0.00	0.00
May tornadoes	**MJO Phase**							
	1	2	3	4	5	6	7	8
Number of tornado days	50	30	27	33	32	45	60	57
Total number of days	72	48	44	49	44	67	92	79
Tornado day likelihood ($\bar{x}$ = 0.68)	0.69	0.63	0.61	0.67	0.73	0.67	0.65	0.72
Tornado day anomaly	0.01	**−0.06**	**−0.07**	−0.01	**0.05**	−0.01	−0.03	**0.04**

[a]Stratified by month and MJO phase, 1990–2011. *p*-values calculated using binomial test statistic. Bold *p* values signify a tornado day likelihood that is statistically significant at the 95% confidence level.

(Figure 2, row 2). During phases 1–4 and phase 8, positive bulk shear anomalies, up to 5 m s^{-1}, were found over the Gulf Coast states and Southern Plains, and negative anomalies, as much as −5 m s^{-1}, were found over the Northern and Central Plains. In phases 5–7, that dipole-like pattern generally reversed, with negative anomalies over the southern domain and positive shear anomalies over the northern domain. Similar to CAPE, these anomalies generally agreed with tornado day anomalies, whereby tornado days were more likely during phases 6 and 8, when bulk vertical wind shear was above normal, and less likely during phases 3–5 and 7, when bulk vertical wind shear was mostly below normal. April anomalies of the normalized product of CAPE and bulk shear highlighted the degree of juxtaposition between CAPE and bulk shear (Figure 2, row 3). For example, phases 3 and 4, associated with below-normal tornado day likelihoods, featured mostly negative anomalies of CAPE and bulk shear, while phases 6 and 8, associated with above-normal

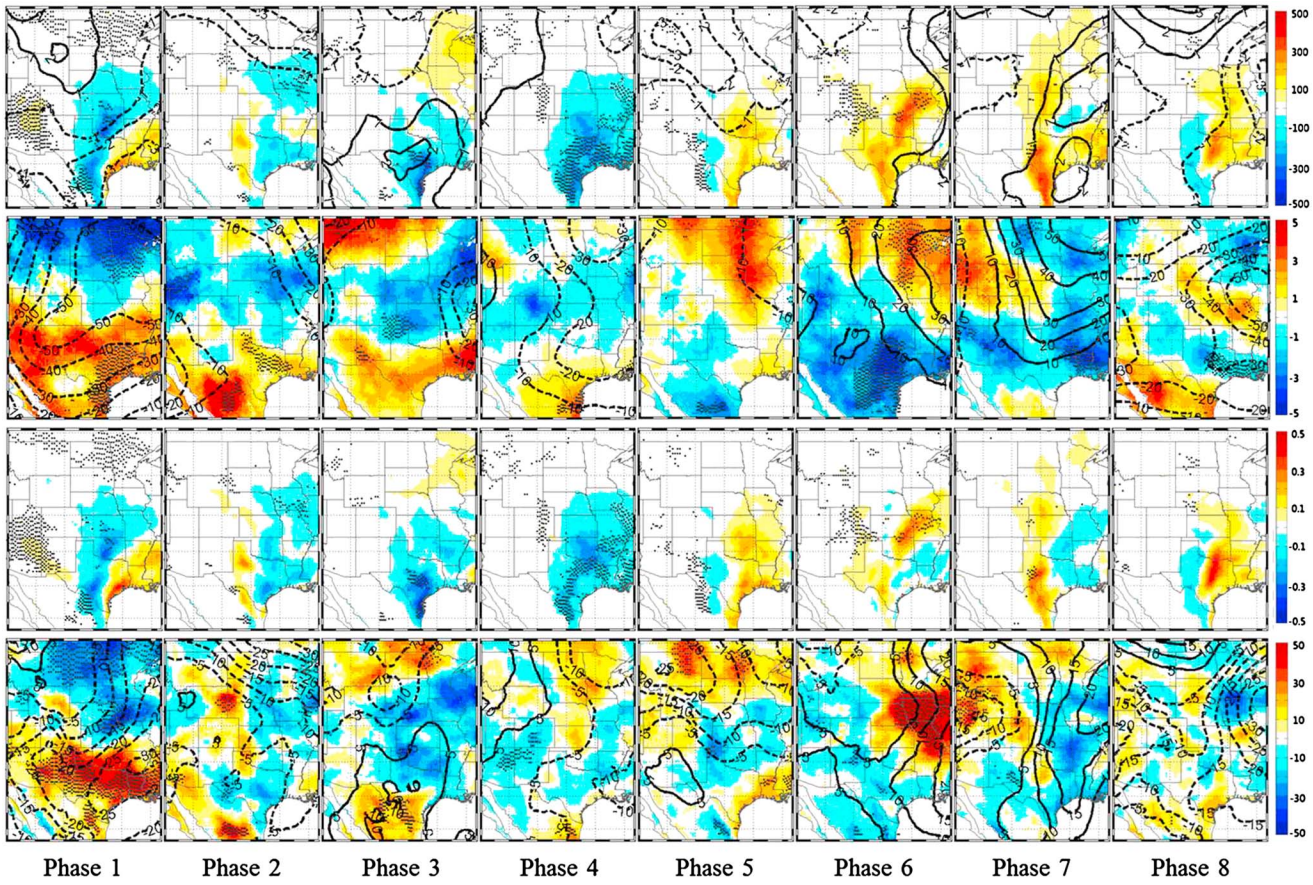

Figure 2. (row 1) Composite anomalies of CAPE in J kg^{-1} and mean sea level pressure in mb; (row 2) 0–6 km bulk vertical wind shear in m s^{-1}, and 500 hPa height in m; (row 3) CAPE multiplied by 0–6 km bulk shear in m^3 s^{-3}, scaled by 20,000; (row 4) and 0–3 km storm-relative helicity in m^2 s^{-2} and 850 hPa height in m, by MJO phase for April 1990–2011. Statistically significant CAPE, bulk shear, and SRH anomalies at 95% confidence indicated by stippling.

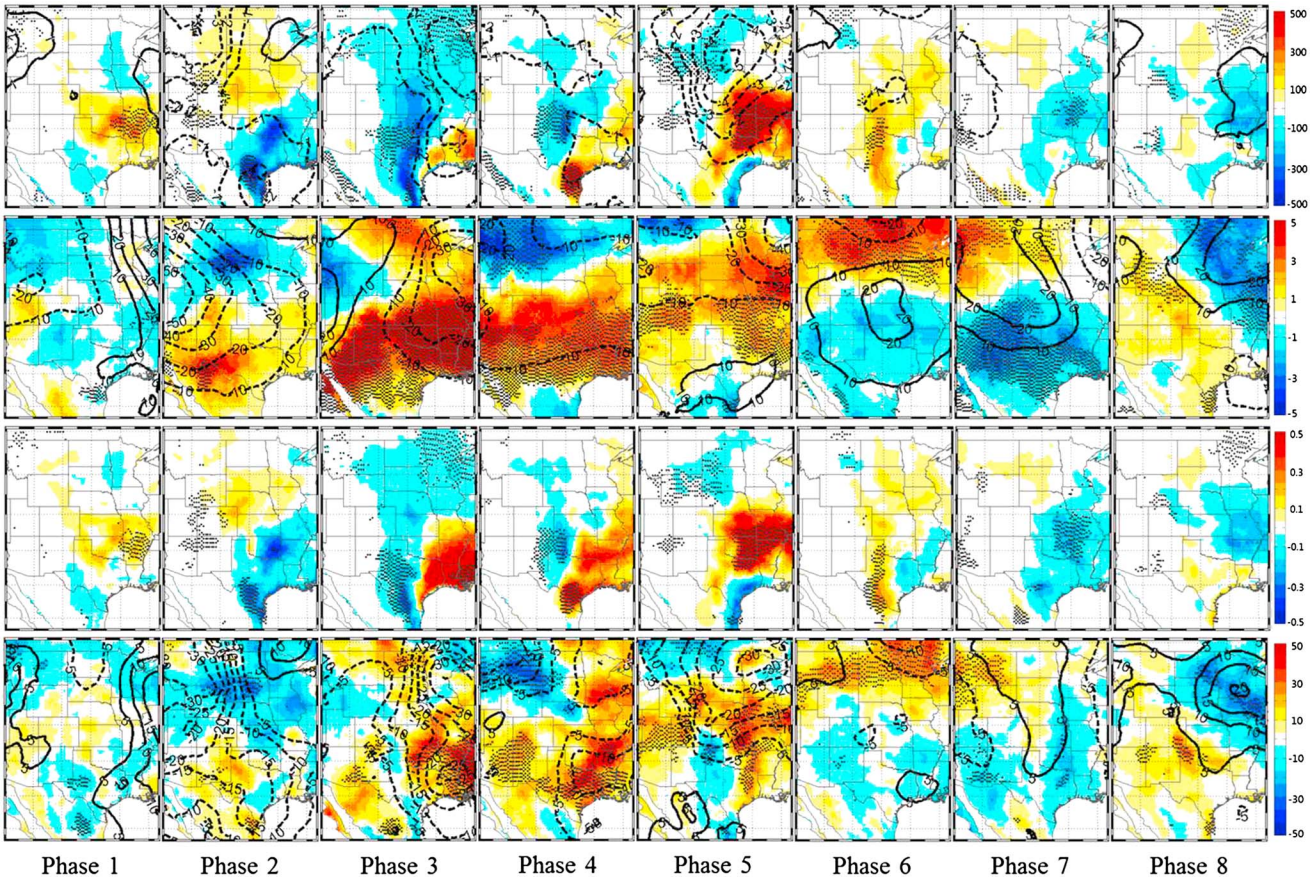

Figure 3. As in Figure 2, but for May.

tornado day likelihoods, featured generally positive anomalies over the domain.

[8] In May, positive CAPE anomalies, up to 500 J kg^{-1}, were found in phase 5 (Figure 3, row 1), in agreement with above-normal tornado day likelihood in that phase. Negative CAPE anomalies, as much as −500 J kg^{-1}, were found during phases 2 and 3, in agreement with below-normal tornado day likelihood during those phases. May bulk wind shear anomalies (Figure 3, row 2), unlike CAPE, had mixed agreement with variability in likelihood of a tornado day. For example, negative bulk shear anomalies in phase 7, and positive anomalies in phase 8, agreed with below- and above-normal tornado likelihood in those phases, respectively, but large regions of positive bulk shear anomalies in phases 2–4 were associated with below-normal tornado day likelihood for those phases. Some clarity into this discrepancy comes through an examination of anomalies of normalized CAPE and bulk shear. For example, phase 5, which had the highest likelihood of a May tornado day, also had a large region of positive normalized CAPE and bulk shear anomalies, and phase 7, with below-normal likelihood of a tornado day, had a large region of negative CAPE and bulk shear anomalies.

[9] Anomaly patterns of 0–3 km SRH in both April and May were less organized than those of CAPE and bulk vertical wind shear, whereby in most phases, both positive and negative SRH anomalies were present, sometimes oriented in a dipole manner. However, there were still several phases when SRH anomaly patterns generally agreed with tornado day anomalies. For instance, in April, a tornado day was more likely during phases 1 and 6, when SRH was mostly above normal, and less likely in phases 3 and 7, when SRH was mostly below normal (Figure 2, row 4). In May, a tornado day was less likely during phase 7, when SRH anomalies were mostly negative, and more likely in phase 8, when SRH anomalies were positive (Figure 3, row 4).

[10] In addition to CAPE, bulk wind shear, and SRH, anomalies of sea level pressure, 500 hPa height, and 850 hPa height were examined, with specific focus on how they might relate to CAPE, bulk vertical wind shear, and SRH. Negative anomalies of sea level pressure tended to be located west of positive CAPE anomalies (Figures 2 and 3, row 1). The surface circulation in response to this pressure field would have had a southerly component in the region of positive CAPE anomalies. Given the low-level moisture and sensible heat source in the Gulf of Mexico, this southerly circulation anomaly would have contributed to positive CAPE anomalies. This pattern was best defined in phase 5 in April (Figure 2) and phase 6 in May (Figure 3). Anomalies of 500 hPa height were similarly associated with bulk vertical wind shear, with negative height anomalies tending to be located west and south of positive bulk shear anomalies, indicating that positive bulk shear anomalies were located downstream of 500 hPa troughs and negative bulk shear anomalies located downstream of 500 hPa ridges. This pattern was seen in most phases in April (Figure 2, row 2) and May (Figure 3, row 2). Anomalies of 850 hPa height were similar in placement and amplitude to those at 500 hPa, and generally, negative 850 hPa height anomalies were located to the west of positive SRH anomalies (Figures 2 and 3, row 4). This indicates that

the lower troposphere circulation response to the height anomalies would contribute to the observed SRH anomalies.

4. Summary and Discussion

[11] We have presented variability in likelihood of a tornado day in the central United States in April and May, stratified by phase of the MJO. This study is one of just a few [e.g., *Thompson and Roundy*, 2013] to examine connections between planetary scale, intraseasonal variability, and microscale weather features, such as tornadoes. We found statistically significant relationships for several phases of the MJO, with likelihood of a tornado day varying by phase in both April and May. In April, tornado days were more likely in phases 6 and 8 and less likely in phases 3–5 and 7. In May, tornado days were more likely in phases 5 and 8 and less likely in phases 2 and 3. This shift in variability from April to May is likely due to the seasonality of the MJO, whereby the meridional propagation speed of circulation anomalies changes as the MJO transitions from projecting onto Northern Hemisphere winter to Northern Hemisphere summer [*Wu et al*., 2006].

[12] Tornado day variability was supported by variability in CAPE, bulk vertical wind shear, and SRH, with environmental conditions known to favor tornado formation occurring more often during phases found to have above-normal tornado day likelihoods. Similarly, environmental conditions known to be unfavorable for tornado formation tended to occur more often during phases found to have below-normal tornado day likelihoods. Furthermore, anomalies of sea level pressure, 500 hPa height, and 850 hPa height generally supported the variability of CAPE, bulk shear, and SRH. Based on these results, we propose the following pathway for the MJO to affect tornadoes: anomalies in intensity and location of tropical deep convection, categorized by the *Wheeler and Hendon* [2004] index, modulated midlatitude circulation patterns. The resulting circulation anomalies, evident in composite plots of 500 hPa height, 850 hPa height, and sea level pressure, in turn modified the local kinematic and thermodynamic environment, seen in anomalies in CAPE, bulk vertical wind shear, and SRH. This environmental variability, in turn, projected onto likelihood of a tornado day. As with other MJO modulations of small-scale weather features, including surface air quality [*Barrett et al*., 2012a] and rainfall in Santiago, Chile [*Barrett et al*., 2012b], composite anomalies of environmental parameters were often noisy, revealing a complex local response to the MJO. One such complex pattern that emerged repeatedly was north-south and NW-SE oriented dipole organization in CAPE, bulk vertical wind shear, and SRH anomalies. Such dipoles suggest that there may be value in further stratifying the tornado data set by geographic area, although such studies would likely have small sample sizes.

[13] Finally, the key result of this study is that the likelihood of a tornado day varies by phase of the MJO. This is similar to the result of *Thompson and Roundy* [2013], although there are several important differences that merit discussion. *Thompson and Roundy* [2013] found that violent tornado outbreaks in March–May occurred most often during phase 2; we found phases 5 (in April) and 8 (in May) to be associated with the highest likelihood of a tornado. This disagreement can be partially explained by differences in methodology, as we did not stratify tornado day by intensity, examined only on April and May, and focused on tornado likelihood for the central United States for the period 1990–2011. *Thompson and Roundy* [2013] examined outbreaks of (E)F-2 and greater tornadoes from March 1974 to May 2010. Based on these methodology differences, our study extends *Thompson and Roundy* [2013] in two important ways. First, by treating April and May separately, we accounted for seasonality in the MJO [*Zhang*, 2005], whereby the teleconnected atmospheric response in North America to deep convection in the tropics changes from April to May. Second, by examining tornadoes of all intensities, we accounted for a more general tornado threat. Given the increasing predictability of the MJO, these results make a significant contribution to our understanding of intraseasonal controls on variability of April–May U.S. tornadoes, a step that is particularly important in improving extended range predictions of tornado activity.

[14] **Acknowledgments.** The authors would like to thank the anonymous reviewers for many helpful comments to improve the manuscript. Partial support for this research came from National Science Foundation grant AGS-1240143.

References

Abatzoglou, J. T., and T. J. Brown (2009), Influence of the Madden-Julian Oscillation on summertime cloud-to-ground lightning activity over the continental United States, *Mon. Weather Rev.*, *137*, 3596–3601.

Barrett, B. S., S. J. Fitzmaurice, and S. R. Pritchard (2012a), Intraseasonal variability of surface ozone in Santiago, Chile: Modulation by phase of the Madden-Julian Oscillation (MJO), *Atmos. Environ.*, *55*, 55–62.

Barrett, B. S., J. F. Carrasco, and A. P. Testino (2012b), Madden-Julian Oscillation (MJO) modulation of atmospheric circulation and Chilean winter precipitation, *J. Clim.*, *25*, 1678–1688.

Becker, E. J., E. H. Berbery, and R. W. Higgins (2011), Modulation of cold-season U.S. daily precipitation by the Madden-Julian Oscillation, *J. Clim.*, *24*, 5157–5166.

Brooks, H. E., J. W. Lee, and J. P. Craven (2003a), The spatial distributions of severe thunderstorm and tornado environments from global reanalysis data, *Atmos. Res.*, *67–68*, 73–94.

Brooks, H. E., C. A. Doswell III, and M. P. Kay (2003b), Climatological estimates of local daily tornado probability for the United States, *Wea. Forecasting*, *18*, 626–640.

Cook, A. R., and J. T. Schaefer, (2008), The relation of El Niño-Southern Oscillation (ENSO) to winter tornado outbreaks, *Mon. Wea. Rev.*, *136*, 3121–3137.

Craven, J. P., H. E. Brooks, and J. A. Hart, (2002a), Baseline climatology of sounding derived parameters associated with deep, moist convection, *Amer. Meteorol. Soc.*, Preprints, 21st Conference on Severe Local Storms, San Antonio, Texas, USA, 643–646.

Davies-Jones, R. P., D. W. Burgess, and M. Foster, (1990), Test of helicity as a tornado forecast parameter, *Am. Meteor. Soc.*, Preprints, 16th Conf. on Severe Local Storms, Kananaskis Park, AB, Canada, 588–592.

Donald, A., H. Meinke, B. Power, A. d. H. N. Maia, M. C. Wheeler, N. White, R. C. Stone, and J. Ribbe (2006), Near-global impact of the Madden-Julian Oscillation on rainfall, *Geophys. Res. Lett.*, *33*, L09704, doi:10.1029/2005GL025155.

Doswell, C. A. III (1987), The distinction between large-scale and mesoscale contribution to severe convection: A case study example, *Wea. Forecasting*, *2*, 3–16.

Doswell, C. A., III, and D. M. Schultz (2006), On the use of indices and parameters in forecasting, *Electronic. J. Severe Storms Meteorol.*, *1*, 1–22.

Doswell, C. A. III, H. E. Brooks, and M. P. Kay (2005), Climatological estimates of daily local nontornadic severe thunderstorm probability for the United States, *Wea. Forecasting*, *20*, 577–595.

Fawbush, W. J., R. C. Miller, and L. G. Starrett (1951), An empirical method of forecasting tornado development, *Bull. Am. Meteorol. Soc.*, *32*, 1–9.

Gensini, V. A., and W. S. Ashley (2011), Climatology of potentially severe convective environments from the North American regional reanalysis, *Electronic J. Severe Storms Meteor.*, *6*, 1–40.

Gottschalck, J., et al. (2010), A framework for assessing operational Madden-Julian Oscillation forecasts: A CLIVAR MJO working group project, *Bull. Am. Meteorol. Soc.*, *91*, 1247–1258.

Jones, C., L. M. V. Carvalho, J. Gottschalck, and W. Higgins (2011), The Madden-Julian Oscillation and the relative value of deterministic forecasts of extreme precipitation in the contiguous United States, *J. Clim.*, *24*, 2421–2428.

Kelly, D. L., J. T. Schaefer, R. P. McNulty, C. A. Doswell III, and R. F. Jr.Abbey (1978), An augmented tornado climatology, *Mon. Weather Rev.*, *106*, 1172–1183.

Kloth, C. M., and R. P. Davies-Jones (1980), The relationship of the 300-mb jet stream to tornado occurrence, NOAA Tech. Memo. ERL NSSL-88, 62 pp.

Lee, J. T., and J. G. Galway (1956), Preliminary report on the relationship between the jet at the 200-mb level and tornado occurrence, *Bull. Am. Meteor. Soc.*, *39*, 217–223.

Lorenz, D. J., and D. L. Hartmann (2006), The effect of the MJO on the North American Monsoon, *J. Clim.*, *19*, 333–343.

Madden, R. A., and P. R. Julian (1971), Description of global-scale circulation cells in the tropics with a 40–50 day period, *J. Atmos. Sci.*, *29*, 1109–1123.

Matthews, A. J., B. J. Hoskins, and M. Masutani (2004), The global response to tropical heating in the Madden-Julian Oscillation during Northern winter, *Q. J. Roy. Meteorol. Soc.*, *130*, 1991–2011.

McCarthy, D. W., (2003), NWS Tornado Surveys and the Impact on the National Tornado Database, Preprints, 1st Symp. F-Scale and Severe-Weather Damage Assessment, Long Beach, CA.

Mesinger, F., and Coauthors (2006), North American regional reanalysis, *Bull. Am. Meteorol. Soc.*, *87*, 343–360.

Rasmussen, E. N. (2003), Refined supercell and tornado parameters, *Wea. Forecasting*, *18*, 530–535.

Rasmussen, E. N., and D. O. Blanchard (1998), A baseline climatology of sounding-derived supercell and tornado forecast parameters, *Wea. Forecasting*, *13*, 1148–1164.

Roundy, P. E., K. MacRitchie, J. Asuma, and T. Melino (2010), Modulation of the global atmospheric circulation by combined activity in the Madden-Julian Oscillation and the El Niño-Southern Oscillation during Boreal winter, *J. Clim.*, *23*, 4045–4059.

Schaefer, J. T. (1986), Severe thunderstorm forecasting: A historical perspective, *Wea. Forecasting*, *1*, 164–189.

Schaefer, J. T., and R. Edwards, (1999), The SPC Tornado/Severe Thunderstorm Database, Preprints, 11th Conf. Applied Climatology, Dallas, TX.

Seo, K. H., and S. W. Son (2012), The global atmospheric circulation response to tropical diabatic heating associated with the Madden-Julian Oscillation during Northern winter, *J. Atmos. Sci.*, *69*, 79–96.

Thompson, R. L., and R. Edwards (2000), An overview of environmental conditions and forecast implications of the 3 May 1999 tornado outbreak, *Wea. Forecasting*, *15*, 682–699.

Thompson, D. B., and P. E. Roundy (2013), The relationship between the Madden-Julian Oscillation and U.S. violent tornado outbreaks in the spring, *Mon. Weather Rev.*, early online release, doi:http://dx.doi.org/10.1175/MWR-D-12-00173.1.

Tippett, M. K., A. H. Sobel, and S. J. Camargo (2012), Association of U.S. tornado occurrence with monthly environmental parameters, *Geophys. Res. Lett.*, *39*, L02801, doi:10.1029/2011GL050368.

Verbout, S. M., H. E. Brooks, L. M. Leslie, and D. M. Schultz (2006), Evolution of the US tornado database: 1954–2003, *Wea. Forecasting*, *21*, 86–93.

Waliser, D. E. (2006), Intraseasonal Variations, in *The Asian Monsoon*, edited by B. Wang, 787 pp., Springer, Heidelberg, Germany.

Wang, B., and H. Rui (1990), Synoptic climatology of transient tropical intraseasonal convection anomalies, *Meteor. Atmos. Phys.*, *44*, 43–61.

Wheeler, M., and H. H. Hendon (2004), An all-season real-time multivariate MJO index: Development of an index for monitoring and prediction, *Mon. Weather Rev.*, *132*, 1917–1932.

Wu, M.-L. C., S. D. Schubert, M. J. Suarez, P. J. Pegion, and D. E. Waliser (2006), Seasonality and meridional propagation of the MJO, *J. Clim.*, *19*, 1901–1921.

Yao, W., H. Lin, and J. Derome, (2011), Submonthly forecasting of winter surface air temperature in North America based on organized tropical convection, *Atmos. Ocean*, *49*, 51–60.

Zhang, C. (2005), The Madden-Julian oscillation, *Rev. Geophys*, *43*, RG2003, doi:10.1029/2004RG000158.

Zhang, C. (2013), Madden-Julian Oscillation: Bridging weather and climate, *Bull. Am. Meteorol. Soc.*, doi:http://dx.doi.org/10.1175/BAMS-D-12-00026.1.

Zhou, S., M. L'Hereux, S. Weaver, and A. Kumar (2011), A composite study of the MJO influence on the surface air temperature and precipitation over the Continental United States, *Clim. Dyn.*, *49*, 1–13.